Curcumin *in vitro* neuroprotective effects are mediated by p62/keap-1/Nrf2 and PI3K/AKT signaling pathway and autophagy inhibition

Xin Li[1]*, Peng Sun[1], Dongmei Zhang[2], Limin Yan[3]*

[1] Department of Neurology, Tangshan Gongren Hospital, Tangshan, Hebei Province, China

[2] Outpatient Department, Tangshan Gongren Hospital, Tangshan, Hebei Province, China

[3] Department of Pathology, Tangshan Gongren Hospital, Tangshan, Hebei Province, 063003, China

* Corresponding author：

Limin Yan, Email: dr_lmyan@163.com

Xin Li, Email: Xinli0315@126.com

Summary

Oxidative stress and autophagy are potential mechanisms associated with cerebral ischemia/reperfusion injury (IRI) and is usually linked to inflammatory responses and apoptosis. Curcumin has recently been demonstrated to exhibit anti-inflammatory, anti-oxidant, anti-apoptotic and autophagy regulation properties. However, mechanism of curcumin on IRI-induced oxidative stress and autophagy remains not well understood. We evaluated the protective effects and potential mechanisms of curcumin on cerebral microvascular endothelial cells (bEnd.3) and neuronal cells (HT22) against oxygen glucose deprivation/reoxygenation (OGD/R) *in vitro* models that mimic *in vivo* cerebral IRI. The cell counting kit-8 (CCK-8) and lactate dehydrogenase (LDH) activity assays revealed that curcumin attenuated the OGD/R-induced injury in a dose-specific manner. OGD/R induced elevated levels of inflammatory cytokines TNF-α, IL-6 as well as IL-1β, and these effects were notably reduced by curcumin. OGD/R-mediated apoptosis was suppressed by curcumin via upregulating B-cell lymphoma-2 (Bcl-2) and downregulating Bcl-associated X (Bax), cleaved-caspase3 and TUNEL apoptosis marker. Additionally, curcumin increased superoxide dismutase (SOD) and glutathione (GSH), but suppressed malondialdehyde (MDA) and reactive oxygen species (ROS) content. Curcumin inhibited the levels of autophagic biomarkers such as LC3 II/LC3 I and Beclin1. Particularly, curcumin induced p62 accumulation and its interactions with keap1 and promoted NF-E2-related factor 2 (Nrf2) translocation to nucleus, accompanied by increased NADPH quinone dehydrogenase (Nqo1) and heme oxygenase 1 (HO-1). Treatment of curcumin increased phosphorylation-phosphatidylinositol 3 kinase (p-PI3K) and p-protein kinase B (p-AKT). The autophagy inhibitor 3-methyladenine (3-MA) activated the keap-1/Nrf2

and PI3K/AKT pathways. This study highlights the neuroprotective effects of curcumin on cerebral IRI.

Keywords: Curcumin; Oxygen glucose deprivation/reoxygenation; Autophagy; Oxidative stress; p62/keap-1/Nrf2; PI3K/AKT

Introduction

The incidence of stroke has increased over the past few decades, and it has now become the second major cause of mortality globally [1]. Stroke is a complex multi-stage process that can be classified into cerebral ischemia and hemorrhagic stroke [2]. Ischemic stroke, the most prevalent stroke subtype, accounts for >80% of all stroke cases [3]. Although reperfusion is required to salvage oxygen-starved tissues, it may further enhance the release of reactive oxygen species (ROS), pro-inflammatory cytokines, and promote post-ischemic capillary no-reflow, aggravating brain damage or dysfunction, which is known as cerebral ischemia/reperfusion injury (IRI). Cerebral IRI is a form of progressive, multifactorial, neurological injury that is associated with inflammatory injury, oxidative damage, and apoptosis [4].

Autophagy is a catabolic process that senses intracellular stress and rapidly induces a response to prevent damage via sequestration as well as degradation of damaged organelles and protein aggregates [5, 6]. Appropriate autophagy protects cells from apoptosis, while in excess, autophagy causes autophagy-associated cell death [7]. LC3II and Beclin-1 are considered autophagosome markers that can regulate the autophagic process [8]. Under normal unstressed states, NF-E2-related factor 2 (Nrf2) is attached by

its inhibitor keap1 predominately in the cytoplasm. In contrast, oxidative stress results in Nrf2-keap1 complex disintegration and Nrf2 translocation into the nucleus, where it binds anti-oxidant response elements (AREs) to initiate the transcription of downstream anti-oxidative genes [9]. The adaptor protein p62 acts as a selective cargo receptor protein for recruiting ubiquitinated proteins and delivering them to autophagosomes for further degradation [10]. When under oxidative stress, p62 can competitively combine with keap1, resulting in Nrf2 dissociation from keap1 and translocation to the nucleus, inducing downstream antioxidant gene expressions [11, 12]. Under the hypoxia context, the transient increase of Nrf2 is crucial in angiogenesis of bEnd.3 cells. The Nrf2 can affect the proliferation, migration and tube formation of bEnd.3 cells via regulating the phosphatidylinositol 3-kinase (PI3K)/protein kinase B (p-AKT) pathway [13]. Also, the PI3K/Akt pathway is involved in the autophagy regulation in response to ROS [14]. Thus, autophagy has potential roles in cerebral ischemia [15].

Curcumin, a major active component in turmeric, is broadly used in both modern and traditional medicine [16]. Recent research has shown that curcumin has anti-apoptotic and anti-inflammatory effects [17-19]. Moreover, curcumin was found to exert powerful antioxidant and neuroprotective effects in Parkinson's disease, cerebral ischemia, and depression [20]. The neuroprotective effects of curcumin are correlated with the brain's autophagy regulation [21]. However, the modulation of curcumin on autophagy and antioxidant effects during cerebral IRI is still not fully understood.

Cerebral microvascular endothelial cells (bEnd.3) are considered as the anatomical basis of the blood–brain barrier (BBB), and the presence of tight junctions contribute to the homeostasis and barrier functions. It has been noticed that IRI disrupts the tight

junctions, leading to the alteration of permeability and brain injury [22]. Compelling evidence has demonstrated that mouse bEnd.3 exposed to oxygen glucose deprivation/reoxygenation (OGD/R) facilitates the study on BBB disruption and therapeutic strategies development after IRI [23]. In this study, we established an *in vitro* OGD/R model of bEnd.3 and neuronal cells (HT22) to explore the influence of curcumin on inflammation, apoptosis, and oxidative stress following IRI. Moreover, we sought to investigate the potential molecular mechanisms through which autophagy interact with keap1/Nrf2 signaling and PI3K/AKT pathway to exert the neuroprotective effects of curcumin.

Material and methods

Cell cultures and OGD/R model induction

The bEnd.3 and HT22 cells were procured from Procell Life Science & Technology Co., Ltd (Wuhan, China) and cultured in Dulbecco's modified Eagle's medium (DMEM) with 10% fetal bovine serum (Grand Island, NY, USA) and 1% penicillin/streptomycin. Cells were incubated in a humidified 5% CO_2 atmosphere maintained at 37°C. For the OGD/R *in vitro* model, bEnd.3 and HT22 cells were incubated in DMEM without glucose and maintained in a 95% (v/v) N_2 and 5% (v/v) CO_2 incubator at 37°C for 6 h. After OGD exposure, the glucose-free DMEM was replaced by high-glucose DMEM, and cells were incubated under normal conditions for appropriate time-points. To evaluate optimal reoxygenation time for OGD/R cell models, five reoxygenation times

were trialed (3, 6, 12, 18, and 24 h) and the cells were compared with those assigned to a control group.

Drug administration

To assess the cellular toxicity effects of curcumin (MedChemExpress, HY-N0005, Figure 1A), bEnd.3 and HT22 cells were exposed to different concentrations (5 μM, 10 μM, 20 μM and 40 μM) of curcumin for 24 h. According to the results of the cytotoxicity assay, bEnd.3 and HT22 cells were pretreated with the non-cytotoxic curcumin doses for 24 h, and thereafter OGD/R was performed. Once the optimal treatment concentration of curcumin was determined, cells were randomized into the following groups: control, curcumin (Cur), OGD/R, and OGD/R+curcumin (OGD/R+Cur). To investigate the effect of curcumin on oxidative damage and excessive autophagy via p62/keap-1/Nrf2 and PI3K/AKT pathways, the autophagy inhibitor 3-methyladenine (3-MA, 6mM) was used in bEnd.3 and HT22 cells.

Cell viability assessment

The cell counting kit-8 (CCK-8) (Beyotime, Shanghai, China) was used for cell viability assessment. Cells were inoculated and cultured in a 96-well plate (5000 cells/well), and exposed to OGD/R or treated with curcumin, after which each well was supplemented with 10 μL CCK-8 solution, followed by a 1-h incubation at 37°C. Absorbance values were determined at 450 nm.

Lactate dehydrogenase (LDH) assay

This assay was conducted using the LDH cytotoxicity assay kit (Thermo Fisher Scientific) according to the manufacturer's instructions. Briefly, 50 μL cell media of

stimulation assays were transferred into 96-well plates. Then, 50 μL of the reaction mixture was added to the wells followed by 30-min incubation at room temperature in the dark. After adding the stop solution, absorbance was determined at 490 nm and 680 nm as a correction wavelength.

Dihydroethidium staining and oxidative indices measurements

Intracellular reactive oxygen species (ROS) were assessed using fluorescently labeled dihydroethidium (DHE). The bEnd.3 cells were seeded into 24-well plates and incubated with a DHE working solution at 37°C for 30 min. Cells were observed under an inverted fluorescence microscope (Olympus, Tokyo, Japan). ROS production in HT22 cells was quantified using the 2,7-dichlorodihydrofluorescein diacetate (DCFH-DA) fluorescent probe. HT22 cells were incubated with DMEM (control) or exposure to OGD/R and curcumin, HT22 cells were harvested and incubated with 10 μM DCFH-DA at 37°C for 30 min in the dark. Intracellular ROS level was measured by flow cytometry (FACScan, BD FACSAria II; BD Company). The level of malondialdehyde (MDA) was assessed by thiobarbituric acid-reactive substances. Glutathione (GSH) and superoxide dismutase (SOD) levels were assessed using GSH and SOD assay kits (Jiancheng Biochemical, Nanjing, China).

Western blot analysis

Proteins were extracted from the bEnd.3 and HT22 cells, and their concentrations were quantitated using a BCA protein assay Kit (Beyotime, Shanghai, China). Proteins (50 μg) were separated by 12% sodium dodecyl-sulfate polyacrylamide gel electrophoresis (SDS-PAGE) and transferred to a polyvinylidene fluoride (PVDF)

membrane, which was then in 5% skim milk at room temperature for 2 h. The membrane was then incubated overnight with the following primary antibodies against Bcl2 (26593-1-AP, Proteintech), Bax (50599-2-Ig, Proteintech), cleaved caspase-3 (WL01992, Wanleibio), p62 (39749, CST), Beclin 1 (3738, CST), LC3 (14600-1-AP, Proteintech), keap1 (60027-1-Ig, Proteintech), Nrf2 (WLH3846, Wanleibio), lamin (12987-1-AP, Proteintech), p-PI3K (ab182651, Abcam), PI3K (ab191606, Abcam), p-AKT (ab38449, Abcam), AKT (ab8805, Abcam) and β-actin (4967, CST) at 4˚C. Following washing using Tris-buffered saline containing 0.1% Tween-20 (0.1% TBST), the membrane was probed with horse radish peroxidase (HRP)-labeled secondary antibody (7074, CST) at RT for 1 h. Quantification of the gray values of the protein bands was done using the ImageJ software (version 2.0.0).

Real-time quantitative PCR (RT-qPCR)

Total RNA isolation and purification from bEnd.3 and HT22 cells were performed using the High Pure RNA extraction kit (Tiangen Biotech Co., Ltd.) in accordance with the manufacturer's instructions. Subsequently, an iScript cDNA Synthesis Kit (Bio-Rad) was used for cDNA synthesis after which RT-qPCR was conducted using the SYBR® green PCR kit (Tiangen Biotech Co., Ltd.). The sequence of primers for qPCR analysis are presented in Table 1. β-actin was used as the internal reference gene for normalization.

Terminal deoxynucleotidyl transferase dUTP nick end labeling (TUNEL) assay

Cellular apoptosis was identified using the terminal deoxynucleotidyl transferase dUTP nick end labeling (TUNEL) detection kit (Beyotime, Shanghai, China). Briefly,

cells were fixed for 30 min with 4% paraformaldehyde and washed using PBS. After permeabilization for 5 min with 0.3% Triton X-100, cells were subsequently washed thrice in PBS. Then, 50 μL TUNEL assay solution was added to the samples followed by incubation in the dark for 60 min at 37°C. Then, cells were sealed with an anti-fluorescence quenching solution and observed under a fluorescence microscopy.

Cell apoptosis measurement

After exposure to OGD/R and treatment of curcumin, HT22 cells (3×10^5) were incubated in 6-well plates and then stained with Annexin V-fluorescein isothiocyanate (FITC)/propidium iodide (PI) using the Annexin V/PI apoptosis detection kit (Biolegend, USA) for 15 min at room temperature as recommended by the manufacturers. Apoptotic cells were determined based on flow cytometry using BeamCyte-1026 cytometer (BeamCyte, China).

Statistical analysis

Data are expressed as mean±SEM. All statistical analyses were performed using the SPSS 23.0 software (IBM Corporation, Armonk, NY, USA). Among-group differences were evaluated by one-way analysis of variance (ANOVA) followed by Duncan's multiple range test. $p<0.05$ was considered to indicate statistical significance.

Results

The effect of Curcumin on cell viability

We first performed time-course experiments to evaluate the impact of reoxygenation time on cell viability. Results of the CCK-8 assay revealed that bEnd.3 cell viability

decreased markedly as reoxygenation time increased and reduced to ~50% 18 h after reoxygenation, with a slight increase after reoxygenation for 24 h (Figure 1B). We next sought to explore the cytotoxic effect of curcumin on bEnd.3 cells. Administration of curcumin at concentrations of 5, 10, and 20 μM exhibited no cytotoxicity, but the highest concentration at 40 μM significantly reduced cell viability (Figure 1C). We also found that curcumin (5, 10, and 20 μM) significantly enhanced the cell viability of OGD/R-treated bEnd.3 cells, partly in a dose-dependent manner (Figure 1D). Moreover, LDH assays showed that curcumin markedly suppressed LDH release (Figure 1E). In HT22 cells, there was a significant decrease in cell viability at 12 h after reoxygenation, while the cell viability was increased at 18 h (Figure 1F). Administration of curcumin at the concentrations of 5 and 10 μM had no cytotoxicity to HT22 cells (Figure 1G) and could significantly reversed OGD/R-induced lower cell viability but inhibited the level of LDH in HT22 cells (Figure 1H-I). Based on these results, bEnd.3 cell were treated with 20 μM curcumin after 18h reoxygenation and HT22 cell were treated with 10 μM after 12h reoxygenation.

Curcumin inhibits inflammatory response and cell apoptosis induced by OGD/R

To evaluate the effect of curcumin on OGD/R-induced inflammatory response, we further determined the products of inflammatory cytokines in bEnd.3 and HT22 cells. There were no significant changes in the levels of IL-6, TNF-α, and IL-1β after the treatment of curcumin in bEnd.3 and HT22 compared with control group. The expression of IL-6, TNF-α, and IL-1β were markedly higher in the OGD/R group than that of the control group, however, curcumin treatment suppressed OGD/R-induced expression of

inflammatory cytokines in bEnd.3 cells (Figure 2A-C). Similar results were observed in HT22 cells (Figure 2D-F).

The expression of apoptosis-related proteins such as the cleavage caspases 3, Bax and Bcl-2 were assessed in bEnd.3 cells by western blotting analysis. The protein levels of cleavage caspases 3 and Bax were significantly elevated after OGD/R induction, while that of antiapoptotic protein Bcl-2 was decreased compared with control group. However, administration of curcumin greatly mitigated these effects (Figure 2G–I). Additionally, TUNEL assay was further performed in bEnd.3 cells to confirm our observation. As shown in Figure 2J-K, OGD/R remarkably elevated the number of TUNEL-positive cells compared with control group, while curcumin inhibited the percentage of apoptotic cells. Meanwhile, the apoptotic HT22 cells were assessed using flow cytometry following curcumin treatment. HT22 cells exposed to OGD/R exhibited higher apoptotic rate than that of control group, whereas curcumin treatment eliminated OGD/R-induced cell apoptosis (Figure 2L-M).

Curcumin abolishes OGD/R-mediated oxidative damage and excessive autophagy

Considering that oxidative stress is associated with autophagic cell death after IRI, we investigated the effect of curcumin on OGD/R-mediated oxidative stress response. DHE immunofluorescence showed that OGD/R significantly enhanced the production of ROS, while curcumin apparently suppressed OGD/R-mediated ROS production (Figure 3A-B). The result showed that OGD/R remarkably increased the level of MDA and suppressed activities of SOD and GSH compared with control group in bEnd.3 cells. In contrast, treatment of curcumin significantly ameliorated the disturbance in oxidative balance by decreasing the product of MDA and increasing the levels of SOD and GSH

compared with OGD/R cells without curcumin treatment (Figure 3C-E). Additionally, to evaluate the inhibitory effect of curcumin on oxidative stress in neurons, the product of ROS was further measured in HT22 cells. As displayed in Figure 3F-G, cells exposed to OGD/R possessed higher ROS level than that of control cells, while administration of curcumin blocked this process.

To further clarify whether OGD/R-induced autophagy, we measured autophagy-related markers such as p62, Beclin-1, and LC3-II/I protein levels in both bEnd.3 and HT22 cells. OGD/R exposure of bEnd.3 cells remarkably induced autophagy, reflected by decreased abundance of p62 and increased LC3-II/LC3-I ratio compared with control group. Higher protein expression of Beclin 1 was also observed in bEnd.3 cells exposed to OGD/R than that of control group (Figure 3H-K). Intriguingly, curcumin treatment significantly decreased protein level of Beclin 1 and LC3-II/LC3-I ratio but elevated the protein level of p62 compared with OGD/R cells (Figure 3H–K). In HT22 cells, OGD/R exposure also induced reduced abundance of p62, increased LC3-II/LC3-I ratio as well as elevated expression of Beclin 1 compared with control group, while curcumin treatment significantly enhanced expression of p62 but decreased LC3-II/LC3-I and Beclin 1 compared with OGD/R-treated HT22 cells (Figure 3L–O).

Curcumin activates the p62-keap1-Nrf2 pathway

To determine whether the keap1-Nrf2 pathway was affected by autophagy after IRI, the protein levels of keap1 and Nrf2 were measured by western blotting in bEnd.3 and HT22 cells. Following OGD/R exposure, the expression of nuclear Nrf2 was significantly decreased in nucleus of bEnd.3 compared with control group, while curcumin enhanced the nuclear translocation of Nrf2 from the cytoplasm; application of autophagy inhibitor

3-MA reversely elevated the nuclear Nrf2 compared with OGD/R group (Figure 4A-B). Keap1 was highly expressed in bEnd.3 cells exposed to OGD/R than those of control cells ($p<0.01$), whereas curcumin treatment significantly suppressed keap1 expression (Figure 4C). In HT22 cells, exposure to OGD/R also inhibited the nuclear translocation of Nrf2 from the cytoplasm and increased keap1 expression (Figure 4D-F). The relative mRNA levels of Nqo1 and HO-1, target genes of Nrf2, were next evaluated by qPCR in bEnd.3 and HT22 cells. The mRNA levels of Nqo1 and HO-1 were remarkably suppressed in the OGD/R group, whereas, expressions of these genes were elevated in curcumin-treated group (Figure 4G-J).

Curcumin activates the PI3K/AKT pathway

Furthermore, we investigated the effect of curcumin on the PI3K/AKT pathway in bEnd.3 and HT22 cells exposed to OGD/R. As it was shown in Figure 5A-C, treatment of curcumin in bEnd.3 cells did not affect the ratio of p-PI3K/PI3K and p-AKT/AKT compared with control group. After exposure to OGD/R, bEnd.3 cells exhibited significant reductions in the ratio of p-PI3K/PI3K and p-AKT/AKT compared with control group, while administration of curcumin notably increased the ratio of p-PI3K/PI3K and p-AKT/AKT compared with OGD/R group. To determine the effect of curcumin on autophagy and PI3K/AKT pathway, the inhibitor of autophagy 3-MA was used in bEnd.3 cells exposed to OGD/R, and application of 3-MA remarkably activated the PI3K/AKT pathway. In consistent with the results from bEnd.3 cells, administration of curcumin as well as 3-MA notably activated the PI3K/AKT pathway compared with HT22 cells exposed to OGD/R (Figure 5D-F).

Discussion

There is accumulating evidence suggesting curcumin has anti-inflammatory, anti-apoptotic, and antioxidant properties and other pharmacological effects. In this study, we observed that the administration of curcumin could reduce the OGD/R-induced secretion of various inflammatory factors, effectively decrease protein expression of apoptosis-related markers, and improve oxidative stress. Moreover, curcumin could prevent OGD/R-induced excessive autophagy. Additionally, we found that curcumin promoted the disassociation of Nrf2 from keap1 and facilitated the nuclear translocation of Nrf2. Also, curcumin activated the PI3K/AKT pathway. These findings demonstrate that curcumin may have the potential to reverse the development of cerebral IRI, which indicates the protective mechanisms of curcumin are associated with the activation of the p62/Keap-1/Nrf2 pathway and PI3K/AKT pathway (Figure 6).

Oxidative stress is a vital mechanism in the pathological processes of IRI [24]. Cerebral IRI leads to mitochondrial integrity disruption and mitochondrial dysfunction, resulting in excessive ROS production and exacerbation of oxidative stress [25]. Down-regulation of ROS levels is an efficient means against OGD/R-induced injury [26]. Curcumin exerts antioxidant effects on brain tissue, such as Alzheimer's and Parkinson's diseases [27, 28]. Wang and colleagues have demonstrated that inhibition of the production of ROS while increasing mitochondrial membrane potential, ATP levels and state 3 respiration can attenuate mitochondrial dysfunction after cerebral IRI [29]. Besides, Zhang et al have deciphered that curcumin exerts inhibitory effects on OGD/R-induced apoptosis and ROS production in SH-SY5Y cells [30]. These findings suggest

that curcumin had potential inhibitory effects on IRI-induced oxidative injury through inhibiting ROS production. Deficiency of SOD impairs mitochondrial function within the neurons of the cerebral cortex, and previous study has revealed that SOD2 mediates the neuroprotective effect of curcumin on OGD/R-induced injury in HT22 cells [31]. Notably, in consistent with previous studies, our data showed that OGD/R treatment enhanced oxidative damage via promoting ROS production as well as increasing MDA levels, inhibited SOD enzyme activity, and decreased the GSH content. Excessive activation of autophagy may cause damage and even death to cells. The dynamic process of LC3 formation and degradation during autophagosome generation, fusion, and degradation can reflect the degree of autophagy [32]. As substrate-bound p62 is degraded by protein hydrolases during lysosomal degradation, elevated p62 levels are often considered a sign of inhibited autophagy [33]. Research has shown that curcumin can influence autophagic regulation to exert neuroprotective effects in neurodegenerative diseases and nerve injury disorders [34]. It has further been reported that acute and severe ischemic injury may lead to excessive activation of autophagy observed through upregulation of Beclin 1, the initiator of autophagy [35]. Another study suggested that autophagy inhibition ameliorates OGD/R-mediated cell damage [36]. Taken together, as we expected, OGD/R exposure obviously evoked autophagy, mirrored by increased Beclin 1 protein levels, the magnitude ratio of LC3-II/LC3-I, and the decreased expression of p62. Curcumin administration rescued OGD/R-induced excessive autophagy.

Autophagy-regulated oxidative stress and apoptosis are associated with cerebral IRI. Recent study showed that ROS production in hypoxic environments is a necessary

stimulus for autophagic induction [37], which is similar to our experimental results. Nrf2 is a dominant transcription factor controlling antioxidant gene expressions. Chu and colleagues have revealed that activation of autophagy regulated by Nrf2 signal pathway mitigates oxidative damage by clarifying damaged organelles and oxidative substances [38]. A previous study has deciphered that activating Nrf2/ARE antioxidant signaling through reducing keap1 can prevent OGD/R-induced oxidative damage in hippocampal neurons [39]. Meanwhile, Rathore et al have showed that administration of curcumin improves rotenone-induced Parkinson's disease via enhancing p62-keap1-Nrf2-mediated autophagy [40]. The recent research has demonstrated that the activation of Nrf2/HO-1 signaling pathway protect HT22 cells from the OGD/R-induced oxidative stress and apoptosis [41]. The aforementioned studies indicate the role of Nrf2 pathway in autophagy-associated oxidative damage. Our study revealed that curcumin treatment enhanced p62-keap1 interaction and promoted nuclear translocation of Nrf2, resulting in accumulated expression of downstream antioxidant enzymes (e.g., Nqo1, and HO-1). Therefore, curcumin is an Nrf2-inducer and is involved in neuroprotective effects through the crosstalk between p62/keap-1/Nrf2 pathway and autophagy, which may share novel insights into therapeutic directions for cerebral IRI from perspective of oxidative stress.

Currently, compelling study has uncovered that the PI3K/AKT pathway plays pivotal role in the regulation of autophagy, apoptosis and inflammation in neurons and activation of PI3K/AKT ameliorates cerebral IRI via suppressing autophagy, apoptotic cells and inflammatory response [42]. Meanwhile, enhancement of PI3K/AKT pathway restores the ROS-induced mitochondrial dysfunction in PC12 cells after exposure to OGD/R [43], suggesting that cerebral IRI-induced oxidative damage is associated with

PI3K/AKT pathway. However, a previous study has demonstrated that application of curcumin attenuates membranous nephropathy through inducing autophagy via the PI3K/AKT/mTOR [44], which is inconsistent with our results. In this study, excessive autophagy was observed in bEnd.3 and HT22 cells after OGD/R exposure and PI3K/Akt pathway was activated by administration of curcumin. Our results indicated that curcumin rescued excessive autophagy to normal level is benefit for cerebral injury. Hence, curcumin may have potentials to alleviate the IRI through PI3K/Akt pathway-mediated proper autophagy.

Nevertheless, there are some limitations in the present study. The autophagic inhibition by 3-MA activates keap-1/Nrf2 pathway and PI3K/AKT pathway, suggesting that curcumin inhibited autophagy may through both keap-1/Nrf2 pathway and PI3K/AKT pathway. The potential interaction between keap-1/Nrf2 pathway and PI3K/AKT pathway may contribute to the cerebral IRI and further experimental studies should be conducted. Although we have demonstrated the neuroprotective effects of curcumin on bEnd.3 and HT22 cells, *in vivo* studies should be performed to validate our results. Whether these keap-1/Nrf2 pathway and PI3K/AKT pathway are involved in other types of cell death is worthy of further investigation to enrich the potential mechanism of curcumin on cerebral IRI.

Our results suggest that curcumin exerts anti-inflammatory as well as anti-apoptotic effects in OGD/R-mediated injury. Moreover, our data showed that autophagy combined with the keap1/Nrf2 and PI3K/AKT functions, which results in protective effect of curcumin against OGD/R-mediated oxidative stress and autophagy. Our findings

facilitate the supplements for the function of curcumin and provide potential targets for cerebral ischemic therapy.

Data availability statement

All data are available from the corresponding author on reasonable request.

Author contributions

Xin Li wrote the manuscript. Xin Li and Peng Sun completed the experiments within the manuscript. Peng Sun and Dongmei Zhang were responsible for data analysis. Limin Yan designed and supervised the experiments.

Conflicts of interest

There is no conflict of interest.

References

1. Mamin FA, Islam MS, Rumana FS, Faruqui F. Profile of stroke patients treated at a rehabilitation centre in Bangladesh. BMC Res Notes 2017;10:520.
2. Zhu H., Wang X, Chen S. Downregulation of MiR-218-5p protects against oxygen-glucose deprivation/reperfusion-induced injuries of pc12 cells via upregulating n-myc downstream regulated gene 4 (NDRG4). Med Sci Monitor 2020;26:e920101.
3. Chen R, Xu XM, Huang LD, Zhong WT, Cui LL. The regulatory role of long noncoding rnas in different brain cell types involved in ischemic stroke. Front Mol Neurosci 2019;12:61.
4. Zhang Z, Sun YH, Chen X. NLRC5 alleviated OGD/R-induced PC12-cell injury by inhibiting activation of the TLR4/MyD88/NF-κB pathway. J Int Med Res

2020;48:300060520940455.

5. Laker RC, Drake JC, Wilson RJ, Lira VA, Lewellen BM, Ryall KA, Fisher CC, Zhang M, Saucerman JJ, Goodyear LJ, Kundu M, Yan Z. Ampk phosphorylation of Ulk1 is required for targeting of mitochondria to lysosomes in exercise-induced mitophagy. Nat Comm 2017;8:548.
6. Shamsaei N, Khaksari M, Erfani S, Rajabi H, Aboutaleb N. Exercise preconditioning exhibits neuroprotective effects on hippocampal CA1 neuronal damage after cerebral ischemia. Neural Regeneration Res 2015;10:1245-1250.
7. Zou HY, Wang LX, Wang MZ, Cheng C, Li S, Shen QY, Fang L, Liu RY. MTOR-Mediated autophagy is involved in the protective effect of ketamine on allergic airway inflammation. J Immunol Res 2019;5879714.
8. Ngwa HA, Kanthasamy A, Gu Y, Fang N, Anantharam V, Kanthasamy AG. Manganese nanoparticle activates mitochondrial dependent apoptotic signaling and autophagy in dopaminergic neuronal cells. Toxicol Appl Pharmacol 2011;256:227–240.
9. Liu W, Chen YH, Meng J, Wu MF, Bi FF, Chang CC, Li H, Zhang LJ. Ablation of caspase-1 protects against TBI-induced pyroptosis in vitro and in vivo. J Neuroinflammation 2018;15(1):48.
10. Bhattacharya S, Yin JG, Winborn CS, Zhang QH, Yue JM, Chaum E. Prominin-1 is a novel regulator of autophagy in the human retinal pigment epithelium. Invest Ophthalmol Vis Sci 2017;58:2366-2387.
11. Ji QQ, Li YJ, Wang YH, Wang Z, Fang L, Shen L, L YQ, Shen LH, He B. Salvianolic acid B improves postresuscitation myocardial and cerebral outcomes in a

murine model of cardiac arrest: involvement of Nrf2 signaling pathway. Oxid Med Cellular Longevity 2020;2020:1605456.

12. Rodriguez-Fernandez IA, Qi Y, Jasper H. Loss of a proteostatic checkpoint in intestinal stem cells contributes to age-related epithelial dysfunction. Nature Comm 2019;10:1050.
13. Huang YJ, Mao Y, Li HY, Shen GX, Nan GX. Knockdown of Nrf2 inhibits angiogenesis by downregulating VEGF expression through PI3K/Akt signaling pathway in cerebral microvascular endothelial cells under hypoxic conditions. Biochem Cell Biol 2018;96:475-482.
14. Kma L, Baruah TJ. The interplay of ROS and the PI3K/Akt pathway in autophagy regulation. Biotechnol Appl Biochem 2022;69:248-264.
15. Sun YM, Zhang T, Zhang Y, Li JF, Jin L, Sun YY, Shi N, Liu KY, Sun XJ. Ischemic postconditioning alleviates cerebral ischemia-reperfusion injury through activating autophagy during early reperfusion in rats. Neurochem Res 2018;43:1826-1840.
16. Hasanzadeh S, Read MI, Bland AR, Majeed M, Jamialahmadi T, Sahebkar A. Curcumin: an inflammasome silencer. Pharmacol Res 2020;159:104921.
17. Bose S, Sarkar N. Natural medicinal compounds in bone tissue engineering. Trends Biotech 2020;38:404-417.
18. Li Y, Li J, Li SS, Wang XX, Liu BL, Fu Q, Ma SP. Curcumin attenuates glutamate neurotoxicity in the hippocampus by suppression of ER stress-associated TXNIP/NLRP3 inflammasome activation in a manner dependent on AMPK. Toxicol Appl Pharmacol 2015;286:53-63.
19. Miao YP, Zhao S, Gao Y, Wang RJ, Wu Q, Wu H, Luo TY. Curcumin pretreatment

attenuates inflammation and mitochondrial dysfunction in experimental stroke: The possible role of Sirt1 signaling. Brain res Bull 2016;121:9-15.

20. Adami R, Bottai D. Curcumin and neurological diseases. Nutritional Neurosci 2022;25:441-461.
21. Forouzanfar F, Read M, Barreto G, Sahebkar A. Neuroprotective effects of curcumin through autophagy modulation. IUBMB Life 2020;72:652-664.
22. Abdullahi W, Tripathi D, Ronaldson PT. Blood-brain barrier dysfunction in ischemic stroke: targeting tight junctions and transporters for vascular protection. Am J Physiol Cell Physiol 2018;315:C343-C356.
23. Li S, Chen J, Liu M, Chen YQ, Wu Y, Li QY, Ma T, Gao JF, Xia Y, Fan MK, Chen A, Lu DB, Su EY, Xu Fei, Chen ZW, Qian JY, Ge JB. Protective effect of HINT2 on mitochondrial function via repressing MCU complex activation attenuates cardiac microvascular ischemia-reperfusion injury. Basic Res Cardiol 2021;116(1):65.
24. Ye N, Zhang NJ, Zhang Y, Qian H, Wu BQ, Sun YX. Cul4a as a new interaction protein of PARP1 inhibits oxidative stress-induced H9c2 cell apoptosis. Oxid Med Cellular Longevity 2019;2019:4273261.
25. Bugger H, Pfeil K. Mitochondrial ROS in myocardial ischemia reperfusion and remodeling. Biochimica et biophysica Acta 2020;1866:165768.
26. Yang TS, Wang QY, Qu YY, Liu Y, Feng CW, Wang YL, Sun WB, Sun ZR, Zhu YL. Punicalin alleviates OGD/R-triggered cell injury via TGF-β–mediated oxidative stress and cell cycle in neuroblastoma cells SH-SY5Y. Evid Based Complement Alternat Med 2021;2021:6671282.
27. Teter B, Morihara T, Lim GP, Chu T, Jones MR, Zuo X, Paul RM, Frautschy SA,

Cole GM. Curcumin restores innate immune Alzheimer's disease risk gene expression to ameliorate Alzheimer pathogenesis. Neurobiol Dis 2019;127:432-448.

28. Ortiz-Ortiz MA, Morán JM, Bravosanpedro, Bravosanpedro JM, González-Polo RA, Niso-Santano M, Anantharam V, Kanthasamy AG, Soler G, Fuentes JM. Curcumin enhances paraquat-induced apoptosis of N27 mesencephalic cells via the generation of reactive oxygen species. Neurotoxicol 2009;30:1008-1018.
29. Wang WW, Xu JP. Curcumin attenuates cerebral ischemia-reperfusion injury through regulating mitophagy and preserving mitochondrial function. Curr Neurovasc Res 2020;17:113-122.
30. Zhang T, Chen XM, Qu YQ, Ding YB. Curcumin alleviates oxygen-glucose-deprivation/reperfusion-induced oxidative damage by regulating miR-1287-5p/LONP2 axis in SH-SY5Y cells. Anal Cell Pathol (Amst) 2021; 2021:5548706.
31. Wang Y, Zhang Y, Yang L, Yuan J, Jia J, Yang S. SOD2 mediates curcumin-induced protection against oxygen-glucose deprivation/reoxygenation injury in HT22 cells. Evid Based Complement Alternat Med 2019;2019:2160642.
32. Zhou YY, Wang ZK, Huang YJ, Bai CJ, Zhang XL, Fang MD, Jun ZY, Liu B. Membrane dynamics of ATG4B and LC3 in autophagosome formation. J Mol Cell Biol 2022;13:853-863.
33. Mathew R, Karp CM, Beaudoin B, Vuong N, Chen GG, Chen HY, Bray K, Reddy A, Bhanot G, Gelinas C, Dipaola RS, Karantza-Wadsworth V, White E. Autophagy suppresses tumorigenesis through elimination of p62. Cell 2009;137:1062-1075.
34. Li WC, Yao SP, Li HR, Meng ZD, Sun XR. Curcumin promotes functional recovery and inhibits neuronal apoptosis after spinal cord injury through the modulation of

autophagy. J Spinal Cord Med 2021;44:37-45.

35. Qian X, Li XJ, Cai QS, Zhang CB, Yu QJ, Jiang YH, Lee, JH, Hawke D, Wang YG, Xia Y, Zheng BH, Liu DX, Jiang T, Lu ZM. Phosphoglycerate kinase 1 phosphorylates beclin1 to induce autophagy. Mol Cell 2017;65:917-931.e6.
36. Xu JJ, Zang YJ, Liu DJ, Yang TW, Wang JL, Wang YJ, Liu XN, Chen DX. DRAM is involved in hypoxia/ischemia-induced autophagic apoptosis in hepatocytes. Aging Dis 2019;10:82-93.
37. Chen L, Liao B, Qi H, Xie LJ, Huang L, Tan WJ, Zhai N, Yuan LB, Zhou Y, Yu LJ, Chen QF, Shu WS, Xiao S. Autophagy contributes to regulation of the hypoxia response during submergence in Arabidopsis thaliana. Autophagy 2015;11:2233-2246.
38. Chu Q, Yu X, Jia R, Wang YX, Zhang YR, Zhang S, Liu YY, Li YL, Chen W, Ye X, Zheng XD. Flavonoids from Apios americana Medikus Leaves Protect RAW264.7 Cells against Inflammation via Inhibition of MAPKs, Akt-mTOR Pathways, and Nfr2 Activation. Oxid Med Cell Longev 2019;2019:1563024.
39. Ren X, Yu J, Guo L, Ma H. TRIM16 protects from OGD/R-induced oxidative stress in cultured hippocampal neurons by enhancing Nrf2/ARE antioxidant signaling via downregulation of Keap1. Exp Cell Res 2020;391:111988.
40. Rathore AS, Singh SS, Birla H, Zahra W, Keshri PK, Dilnashin H, Singh R, Singh S, Singh SP. Curcumin Modulates p62–Keap1–Nrf2-Mediated Autophagy in Rotenone-Induced Parkinson's Disease Mouse Models. ACS Chem Neurosci 2023.
41. Zhang Q, Wang J, Zhang HL, Zeng T. Dihydromyricetin inhibits oxidative stress and apoptosis in oxygen and glucose deprivation/reoxygenation-induced HT22 cells by

activating the Nrf2/HO-1 pathway. Mol Med Rep 2021;23:1-8.

42. Liu Y, Qu XN, Yan MJ, Li DL, Zou R. Tricin attenuates cerebral ischemia/reperfusion injury through inhibiting nerve cell autophagy, apoptosis and inflammation by regulating the PI3K/Akt pathway. Hum Exp Toxicol 2022;41:09603271221125928.
43. Chen MH, Lu Y, Zhou M, Wang WL, Zheng MZ, Liu CM. The protection impact of tectoridin on PC12 cell preventing OGD/R-caused damage through PI3K/AKT signaling channel. Eur J Pharmacol 2023:175491.
44. Tu DQ, Jin J, Hu X, Ren Y, Zhao L, He Q. Curcumin improves the renal autophagy in rat experimental membranous nephropathy via regulating the PI3K/AKT/mTOR and Nrf2/HO-1 signaling pathways. Biomed Res Int 2020;2020:7069052.

Figures

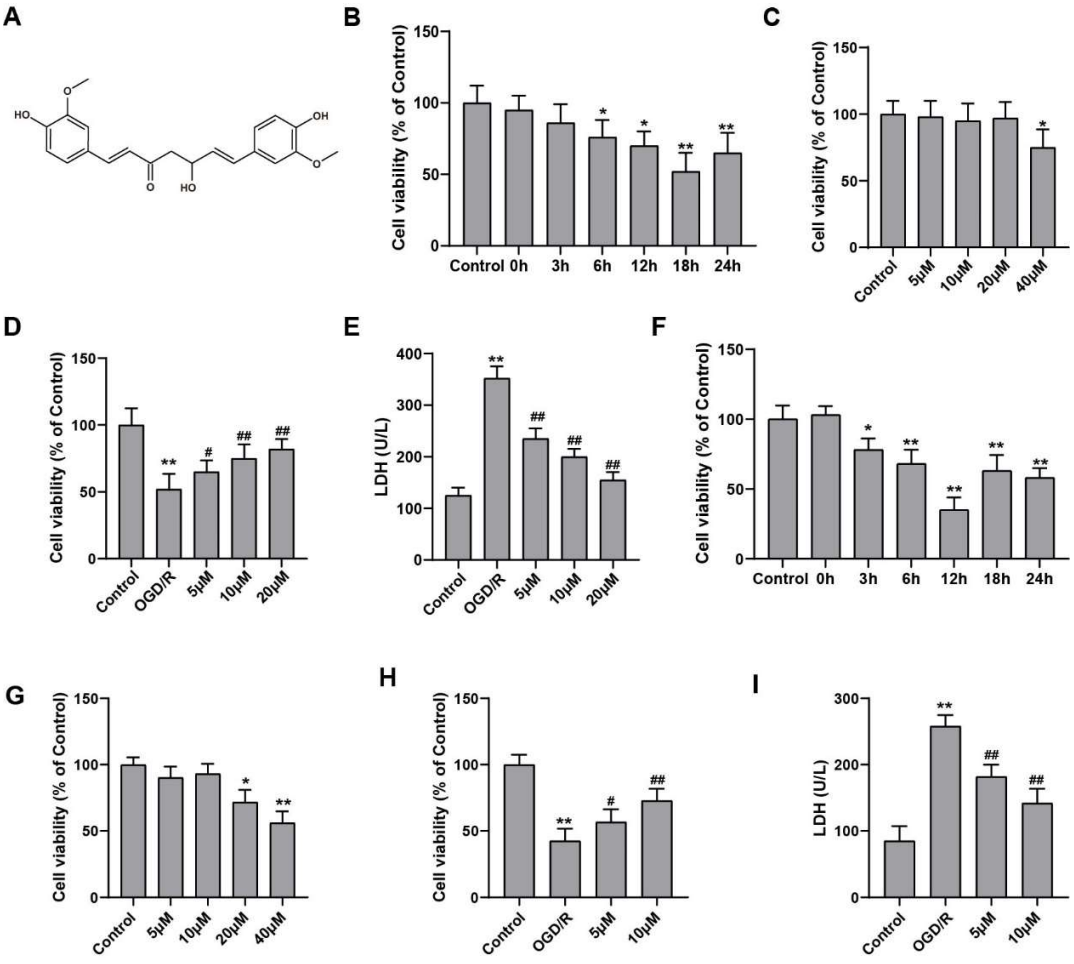

Figure 1. Effects of curcumin on cell viability and LDH release after OGD/R exposure in bEnd.3 and HT22 cells. (A) Chemical structure of curcumin. (B) Reoxygenation time determination in bEnd.3 cells. (C) Effects of different concentration of curcumin (40, 20, 10, and 5 μM) on cell viability before OGD/R induction in bEnd.3 cells. (D) Administration of curcumin (5, 10, and 20 μM) enhances cell viability and (E) inhibits

LDH release in bEnd.3 cells. (F) Reoxygenation time determination in HT22 cells. (G) Effects of different concentration of curcumin (40, 20, 10, and 5 μM) on cell viability before OGD/R induction in HT22 cells. (H) Administration of curcumin (5 and 10μM) enhances cell viability and (I) decreases LDH release in HT22 cells. *$p<0.05$ and **$p<0.01$ vs control. #$p<0.05$ and ##$p<0.01$ vs OGD/R.

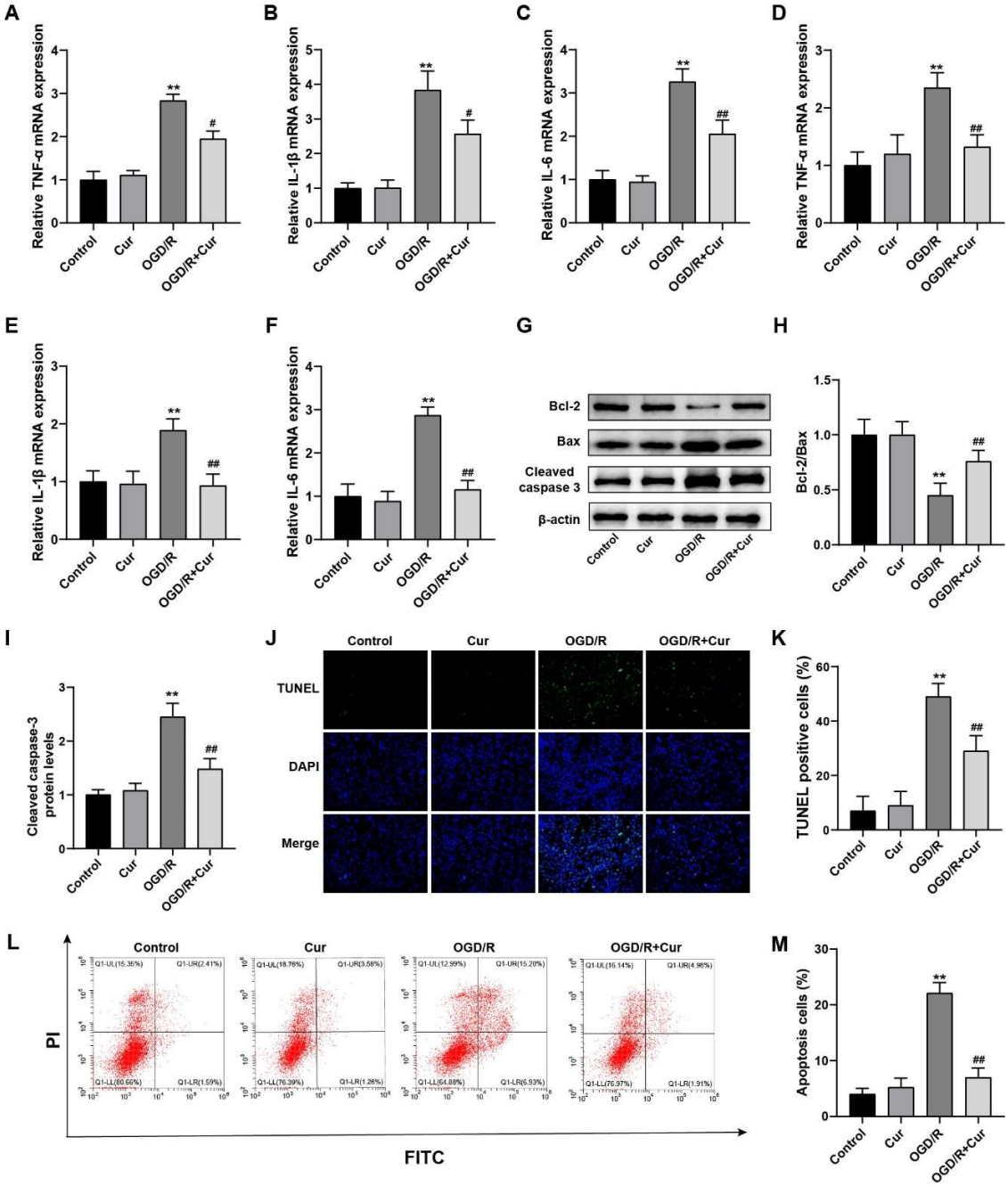
A
Relative TNF-α mRNA expression
B
Relative IL-1β mRNA expression
C
Relative IL-6 mRNA expression
D
Relative TNF-α mRNA expression
E
Relative IL-1β mRNA expression
F
Relative IL-6 mRNA expression
G
Bcl-2
Bax
Cleaved caspase 3
β-actin
H
Bcl-2/Bax
I
Cleaved caspase-3 protein levels
J
Control
Cur
OGD/R
OGD/R+Cur
TUNEL
DAPI
Merge
K
TUNEL positive cells (%)
L
PI
FITC
M
Apoptosis cells (%)

Figure 2. Curcumin ameliorates OGD/R-induced inflammatory cytokines and apoptosis in bEnd.3 and HT22 cells. (A-C) The relative expressions of TNF-α, IL-1β and IL-6 after curcumin treatment in bEnd.3 cells exposed to OGD/R. (D-E) The relative expressions of TNF-α, IL-1β and IL-6 after curcumin treatment in HT22 cells exposed to OGD/R. (G) Representative blots of apoptosis-related proteins (Bcl-2, cleaved caspase-3 and Bax) in bEnd.3 cells. Statistical graphs of relative protein levels of Bcl-2/Bax (H) and cleaved caspase-3 (I). (J) Representative images for TUNEL staining for bEnd.3 cells. (K) Statistical graphs of apoptosis cells (% of DAPI). (L) Representative flow cytometry plots for apoptotic HT22 cells and (M) histograms for apoptotic cell rates after exposure to OGD/R and treatment of curcumin. **$p<0.01$ and ***$p<0.001$ vs control. #$p<0.05$ and ##$p<0.01$ vs OGD/R.

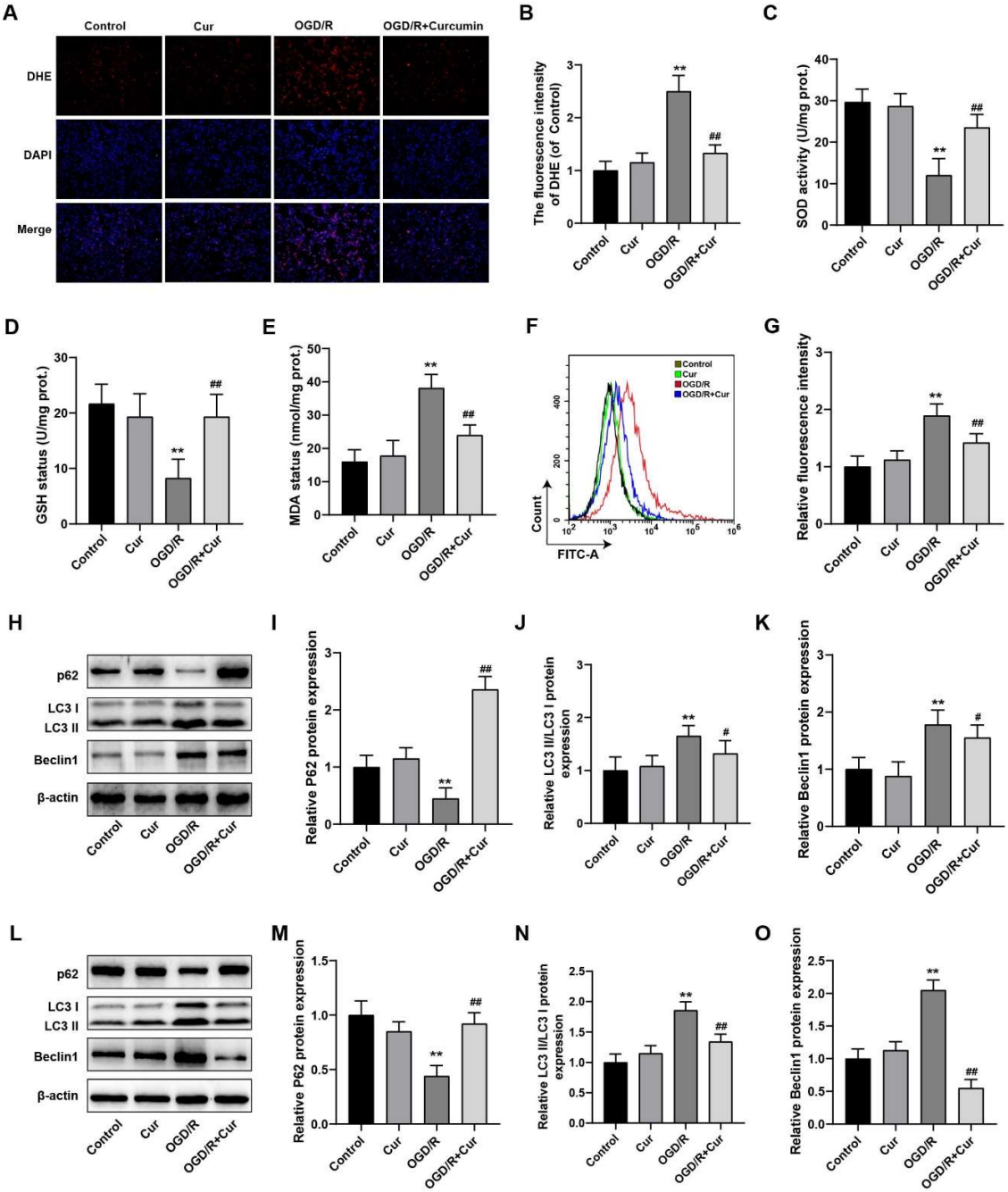
A
Control
Cur
OGD/R
OGD/R+Curcumin
DHE
DAPI
Merge
B
The fluorescence intensity of DHE (of Control)
C
SOD activity (U/mg prot.)
D
GSH status (U/mg prot.)
E
MDA status (nmol/mg prot.)
F
Control
Cur
OGD/R
OGD/R+Cur
Count
FITC-A
G
Relative fluorescence intensity
H
p62
LC3 I
LC3 II
Beclin1
β-actin
I
Relative P62 protein expression
J
Relative LC3 II/LC3 I protein expression
K
Relative Beclin1 protein expression
L
M
N
O

Figure 3. Curcumin ameliorates OGD/R-induced oxidative stress and excessive autophagy in bEnd.3 and HT22 cells. (A) Representative images of dihydroethidium (DHE) for measuring the production of ROS. Red represents the content of ROS in bEnd.3 cells. (B) Histograms for DHE-positive bEnd.3 cells after exposure to OGD/R and treatment of curcumin. The activity of SOD (C), the level of GSH (D) and the production of MDA (E) after exposure to OGD/R and treatment of curcumin. (F) Representative images for DCFH-DA measuring the production of ROS in HT22 cells. (G) Histograms for fluorescence intensity of ROS in HT22 cells after exposure to OGD/R and treatment of curcumin. (H) Representative western blot bands for autophagic biomarkers p62, LC3-II/ LC3-I and Beclin 1 in bEnd.3 cells. (I-K) Histograms for p62, LC3-II/ LC3-I and Beclin 1 in bEnd.3 cells. (L) Representative western blot bands for p62, LC3-II/ LC3-I and Beclin 1 in HT22 cells. (M-O) Histograms for p62, LC3-II/ LC3-I and Beclin 1 in HT22 cells. **$p<0.01$ vs control, #$p<0.05$ and ##$p<0.01$ vs OGD/R.

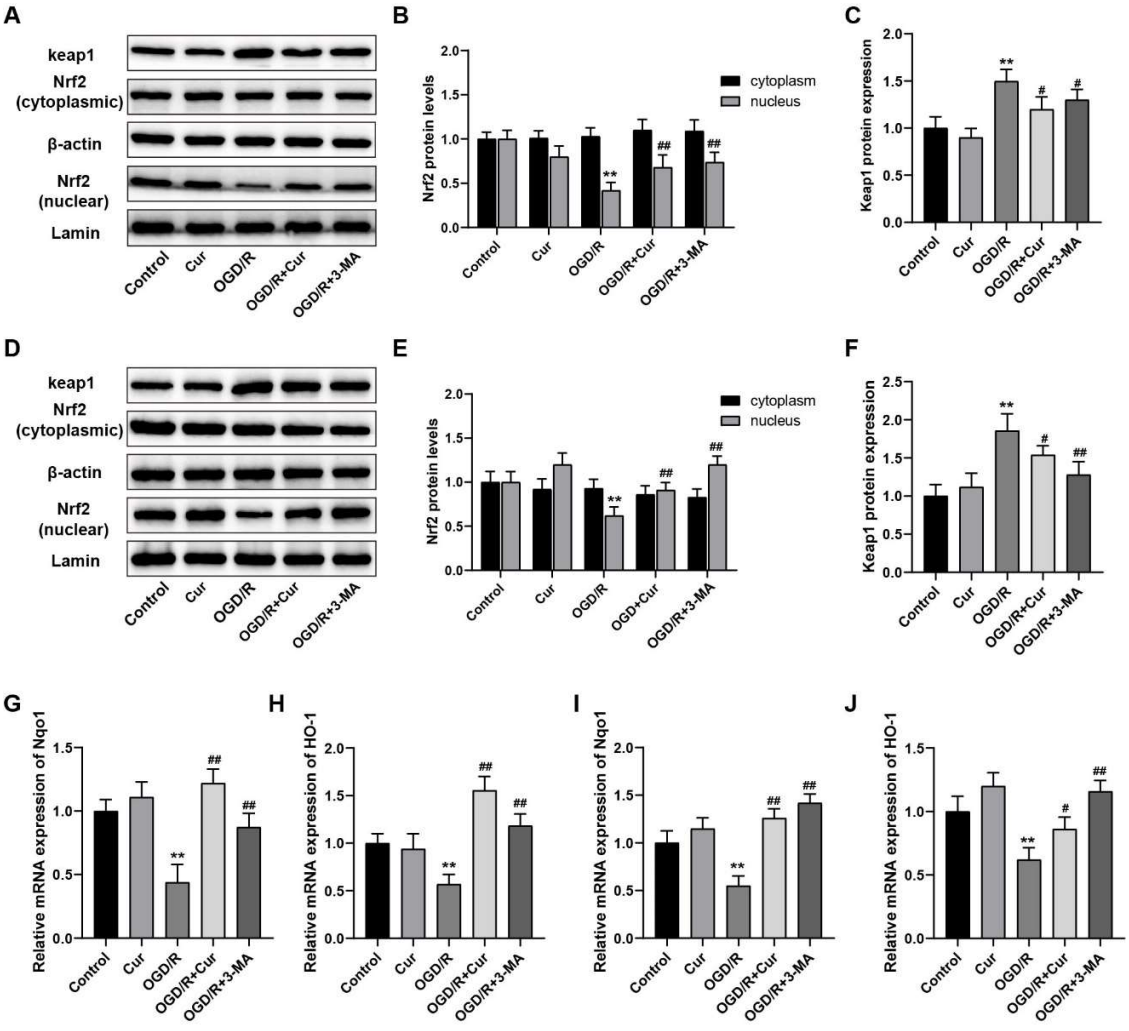

Figure 4. Curcumin activates the p62/Keap-1/Nrf2 signaling pathway in bEnd.3 and HT22 cells. (A) Representative western blot bands for keap1, nuclear Nrf2 and cytoplasmic Nrf2 in bEnd.3 cells after exposure to OGD/R and treatment of curcumin/3-

MA. (B-C) Histograms for protein levels of nuclear and cytoplasmic Nrf2 as well as keap1 in OGD/R-induced and curcumin/3-MA-treated bEnd.3 cells. (D) Representative western blot bands for keap1, nuclear Nrf2 and cytoplasmic Nrf2 in HT22 cells. (E-F) Histograms for protein levels of nuclear and cytoplasmic Nrf2 as well as keap1 in OGD/R-induced and curcumin/3-MA-treated HT22 cells. (G-H) The mRNA levels of Nqo1 and HO-1 in OGD/R-induced and curcumin/3-MA-treated bEnd.3 cells. (I-J) The expression of Nqo1 and HO-1 in OGD/R-induced and curcumin/3-MA-treated HT22 cells. **$p<0.01$ vs control. #$p<0.05$ and ##$p<0.01$ vs OGD/R.

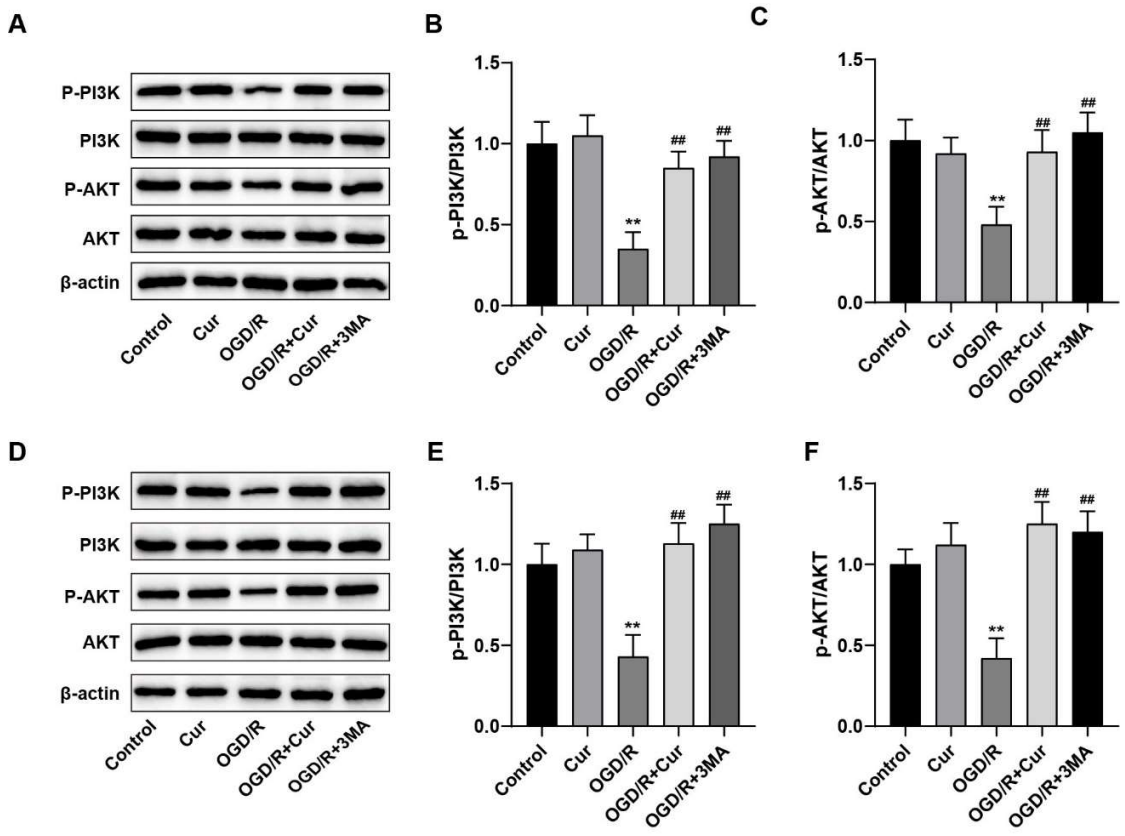

Figure 5. Curcumin activates the PI3K/AKT pathway in bEnd.3 and HT22 cells. (A) Representative western blot bands for p-PI3K, PI3K, p-AKT and AKT in OGD/R-induced and curcumin/3-MA-treated bEnd.3 cells. (B-C) Histograms for the ratio of p-PI3K/PI3K and p-AKT/AKT in bEnd.3 cells. (D) Representative western blot bands for p-PI3K, PI3K, p-AKT and AKT in OGD/R-induced and curcumin/3-MA-treated HT22

cells. (E-F) Histograms for the ratio of p-PI3K/PI3K and p-AKT/AKT in HT22 cells. **p<0.01 vs control. ##p<0.01 vs OGD/R.

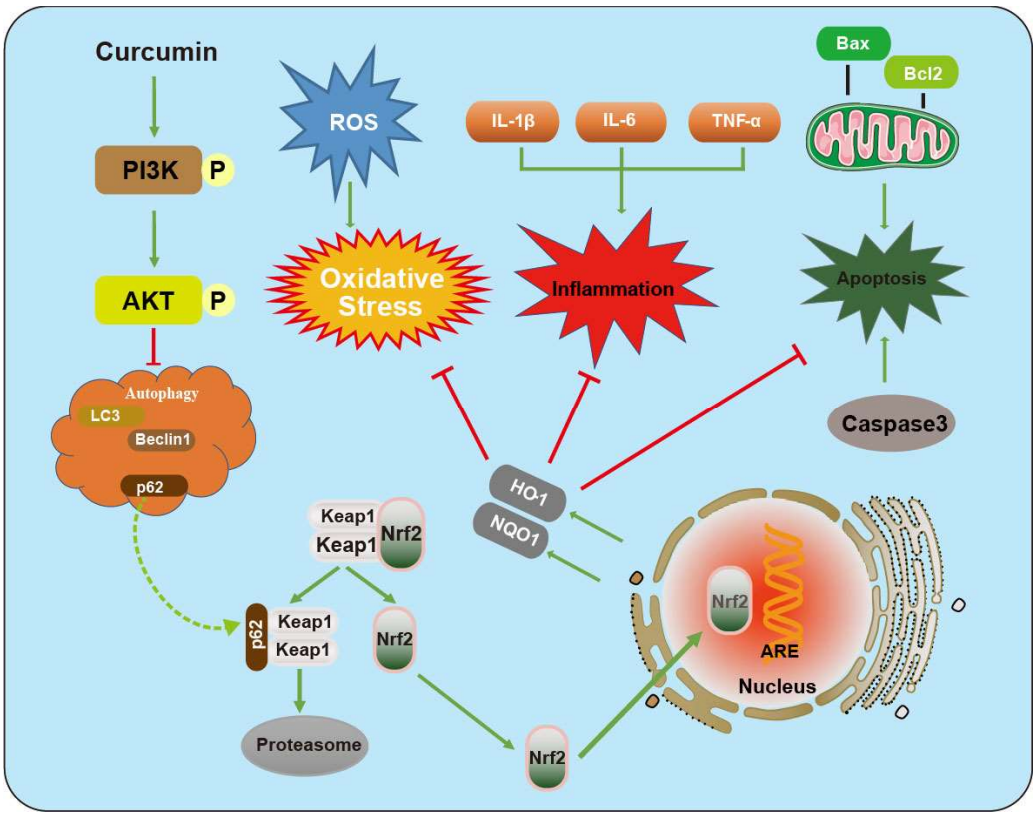

Figure 6. Potential mechanisms of curcumin against OGD/R-induced cell damage in by regulating inflammation, apoptosis, oxidative stress, p62/Keap-1/Nrf2 pathways and PI3K/AKT pathway.

Table

Table 1. Primer sequences used for RT-PCR analysis.

Gene	Forward primer sequence, 5'-3'	Reverse primer sequence, 5'-3'
TNF-α	GGTGCCTATGTCTCAGCCTC	CAGATTGACCTCAGCGCTGA
IL-1β	GTGGCAGCTACCTGTGTCTT	CTCTGCTTGTGAGGTGCTGA
IL-6	GCCTTCTTGGGACTGATGCT	GCCACTCCTTCTGTGACTCC
Nqo1	GTCCATTCCAGCTGACAACCA	TTGCCCTGAGGCTCCTAATC
HO-1	TGCTAGCCTGGTGCAAGATA	GCCAACAGGAAGCTGAGAGT
β-actin	CTTCCAGCCTTCCTTCCTGG	TTCTGCATCCTGTCGGCAAT